Surface bond enhancement, stress and reconstruction on Au(100)

1989 J. Phys.: Condens. Matter 1 3645

(http://iopscience.iop.org/0953-8984/1/23/008)

J. Phys.: Condens. Matter **1** (1989) 3645–3654. Printed in the UK

Surface bond enhancement, stress and reconstruction on Au(100)

James F Annett† and J E Inglesfield‡

† Department of Physics, University of Illinois at Urbana-Champaign, 1110 W. Green St., Urbana, IL 61801, USA

‡ Daresbury Laboratory, Science and Engineering Research Council, Daresbury, Warrington WA4 4AD, UK

Received 7 October 1988

Abstract. The (100) and (111) surfaces of gold reconstruct in such a way as to increase the density of surface atoms, this being thought to result from large tensile stresses in the ideal surfaces. We present self-consistent electronic structure calculations of unreconstructed Au(100) using the surface embedded Green function approach. The surface charge density shows increased bond-charge in the first and second layers which, by a Hellmann–Feynman theorem, leads to attractive surface stresses. This enhancement of surface bonds is shown to be a quite general property of s-band metals and is a consequence of surface band narrowing. The same features are included implicitly in the 'glue model' which has proved successful in describing gold reconstructions.

1. Introduction

The structural and chemical properties of transition-metal surfaces remain poorly understood despite their great technological importance. Even the surfaces of gold, which should be relatively simple because of the full d shell and uncomplicated Fermi surface, exhibit unusual surface reconstructions. For example the Au(110) surface reconstructs in a (1×2) 'missing row' structure [1]. The Au(111) surface has a $(23 \times \sqrt{3})$ reconstruction corresponding to a compressed surface layer in which 24 surface atoms occupy 23 bulk lattice spacings [2]. Similarly the Au(100) surface exhibits a dominant (1×5) behaviour with a 20% increase in density relative to that of the bulk [3]. Superimposed on this structure are long period incommensurate modulations [4], of which the dominant periods have been variously interpreted as (20×5) [5], c(26×68) [6] or a rotated hexagonal structure [7] $\left[\begin{smallmatrix} 26 & 0 \\ z & 48 \end{smallmatrix}\right]$ where $-5 \leqslant Z \leqslant 0$.

At present we do not have a complete theoretical understanding of these various reconstructions in terms of the electronic structure and chemical bonding at the surface. The most successful theoretical model to date is the so-called 'glue model' in which the energy is parametrised in terms of a pair potential and a many-atom 'glue' term

$$E = \sum_{i<j} \phi(|\boldsymbol{r}_i - \boldsymbol{r}_j|) + \sum_i U(n_i) \tag{1}$$

where

0953-8984/89/233645 + 10 $02.50

$$n_i = \sum_{j,i \neq j} \rho(|\boldsymbol{r}_i - \boldsymbol{r}_j|). \tag{2}$$

By fitting the functions $\phi(r)$, $U(n)$ and $\rho(r)$ to various experimental quantities, Ercolessi, Tosatti and Parrinello [8] were able to give a good description of the $(M \times 5)$ Au(100) reconstruction with $M \simeq 34$. The same model predicts the missing-row reconstruction of Au(110) [9]; similar calculations for Pt(110) [10] also found that the missing-row structure was the most stable, as seen experimentally [11]. First principles effective medium calculations [12], which are closely related to equations (1) and (2), predicted the (2×1) Au(110)-reconstruction and found that Cu(110) and Ag(110) were stable.

The classic *ab initio* method for determining minimum energy surface geometries is to perform total energy calculations. These have proved successful in predicting the Au(110) missing-row reconstruction [13]. Unfortunately this method is unable to treat the very large unit cells encountered in the reconstructed Au(111) and (100) surfaces. One alternative approach for these surfaces has been to carry out first-principles calculations for the ideal surfaces and then to assess the stability of the surface towards reconstruction. A key concept here is the idea of surface stress, defined as the strain derivative of the surface energy [14, 15]

$$g_{\alpha\beta} = \frac{1}{A} \frac{\partial(A\gamma)}{\partial \varepsilon_{\alpha\beta}} \tag{3}$$

where γ is the surface energy per unit area, A is the area and $\varepsilon_{\alpha\beta}$ is the 2D strain tensor of the surface. Since both the surfaces Au(100) and Au(111) reconstruct in a way that increases the density of surface atoms, one might expect that the reconstruction is driven by a large stress in the unreconstructed surface. Indeed *ab initio* pseudopotential calculations for Au(111) [16] showed a stress of $0.173\,\text{eV}\,\text{Å}^{-2}$ compared with $0.078\,\text{eV}\,\text{Å}^{-2}$ on Al(111) [15], which suggests that these may give a valid picture. However, the connection between the stress and the reconstruction remains far from clear since other factors, such as the discommensuration energy of the surface layer, must play a role in determining the stability of the surface. For example, even larger surface stresses were found on Pt(111) and Ir(111), these being 0.350 and 0.331 eV Å^{-2} respectively [16], although these surfaces appear more stable than Au(111).

In this paper we shall examine the Au(100) surface from a different approach. Firstly we shall present first-principles electronic structure calculations of the surface. We shall then use the densities of states (DOS) and charge density of the surface to build up a detailed picture of the bonding, especially the interplay between sp free electron behaviour, the d–d closed shell overlap and the s–d hybridisation at the surface. By considering the flow of the charge density at the surface relative to the bulk (following the approach of Heine and Marks [17]), we can establish that the surface bonds are stronger than those in the bulk, and thus contribute to a positive (tensile) surface stress. Enhanced surface bonding is shown to be a quite general property of s-band metals. The many-body term in the glue model (equation 2) also describes the same phenomenon, hence explaining the success obtained with that model.

2. Surface-embedded Green function calculations

In order to understand the bonding in the Au(100) surface we have performed self-consistent local-density functional calculations using the surface-embedded Green func-

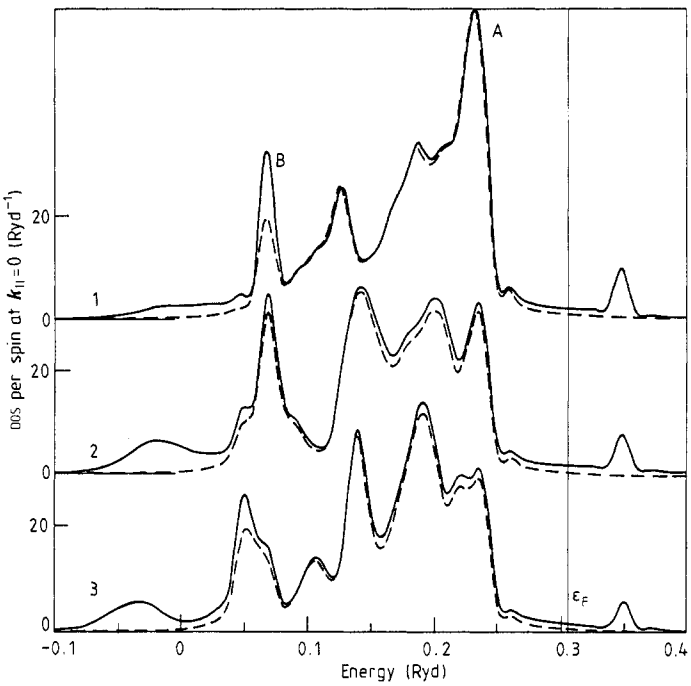

Figure 1. Muffin-tin density of states (DOS) at zero parallel wavevector ($\boldsymbol{k}_{\parallel} = 0$) for the top three layers on Au(100), labelled 1, 2 and 3, respectively. The broken curves show the d-only muffin-tin DOS. The Fermi energy ε_F is at 0.3059 Ryd. See § 2 of text for a discussion of surface resonance peaks A and B.

tion method (SEGF) [18]. In this approach, the Kohn–Sham wavefunctions are calculated in a true surface geometry without any slab or supercell approximations, this being achieved by solving Schrödinger's equation in the surface region with the boundary conditions at the bulk interface given by a surface 'embedding' potential. The embedding potential represents the scattering properties of the bulk solid and can be calculated from the bulk Green function. In general the embedding potential is complex and energy dependent, which ensures that the DOS in the surface region is in principle exact, unlike in a finite slab calculation. In our calculations we included one, two or three atoms explicitly in the surface region. In each case the work function converged to 5.74 eV, compared to the experimental value of 5.47 eV. We used the LAPW basis set implementation of the SEGF method, described in more detail in [18], with 80, 100 and 150 LAPW basis functions for the 1, 2 and 3 atom calculations, respectively. The calculations were scalar-relativistic, employing the Hedin–Lundqvist exchange-correlation potential.

Figure 1 shows the density of states per spin at $\boldsymbol{k}_{\parallel} = 0$ in each muffin tin of the three-atom calculation. The broken curve shows the d-electron contribution only. The most prominent surface features are: firstly a general narrowing of both the s- and d-band DOS, visible in the reduced s weight between −0.1 and 0 Ryd and in the much more peaked d-only DOS. In addition to this, a well defined peak appears at the upper edge of the d band, labelled A. This can be thought of as a surface resonance almost split off from the bulk d band. A local orbital analysis of a similar peak on Ni(100) shows that it can be attributed to the $3z^2 - r^2$, xz and yz d states, the energy of which is raised by the surface [19]. A second peak, labelled B in figure 1, appears at the bottom edge of

the d band. This peak has mixed s and d character with the amount of s weight increased and the d weight decreased at the surface, reflecting the increased s–d hybridisation at the surface because of the lower symmetry.

More information on the surface can be obtained from the integrated muffin DOS per spin for s, p or d symmetry. The total occupied d weights within the muffin tin are 4.47, 4.46 and 4.47 in the top, second and third layers respectively. Since the d density remains constant, clearly, whatever increased sp–d hybridisation is occurring at the surface only involves coupling between occupied states, and is not significantly increasing the coupling of occupied d states with the unoccupied bands. The combined s and p weights are 0.48, 0.54, 0.54 in the top three layers, respectively. This reduction in the sp integrated DOS at the surface implies that s–p band-like states are perturbed so they have less weight in the surface muffin tin and more in the interstitial and vacuum regions. We shall see this redistribution again in the charge density plots.

What can we conclude about the surface bonding from these observations? The bulk cohesive properties of gold can be understood as a combination of three factors: firstly there is s–p free electron bonding, secondly there is overlap repulsion between the closed d shells, and finally there is an attractive contribution due to s–d hybridisation. From the constancy of the d muffin-tin weight we can conclude that increased s–d hybridisation does not play a large role in determining the surface energy since it mostly involves coupling between occupied states which would give no net total energy change. The d–d repulsion is not expected to be very different at the surface since the d wavefunctions will be atom-like and not very sensitive to the local environment. That leaves s–p bonding as the main factor in determining the surface properties. We shall argue below that the changed s–p bonding at the surface, combined with the fixed d–d repulsion, leads to the unusual surface reconstructions.

3. Self-consistent charge density

It has been argued [17] that the origin of the reconstructions of gold can be understood in terms of the redistribution of charge that takes place at the surface. Firstly, it was argued that the charge density relaxes both tangentially and normal to the surface, driven by the difference between the s–p electron-gas pressure and the d–d repulsion at the surface. Secondly, the predicted charge flow was used together with the Hellmann–Feynman theorem to find both the directions of the stress on the clean surface and of the forces on atoms at steps. In this section we shall consider the self-consistent charge density and compare it to the Heine-Marks model [17].

Figures 2 and 3 show the self-consistent charge density of the gold surface in the (10) and (11) surface directions. As a guide to the eye, the bulk Wigner–Seitz cell boundaries have been superimposed. Superficially the charge density plot is not very different from one due to simple superposition of atomic densities (shown in figure 4 for the (10) direction), but a closer inspection reveals important features of the bonding. The most noticeable of these is that the outer contours of the atoms are not quite spherical but are elongated towards the nearest neighbours. This is due to the bond charge between the atoms, and is present for both bulk and surface atoms.

Using the Wigner–Seitz cell boundaries shown in figures 2 and 3 as a guide we can see where the charge flows do indeed take place at the surface, compared to simple truncation of the bulk density. Clearly there is less charge in regions A and B in figure 2 (and A′ and B′ in figure 3) compared with the sub-surface atoms (e.g. region D). The

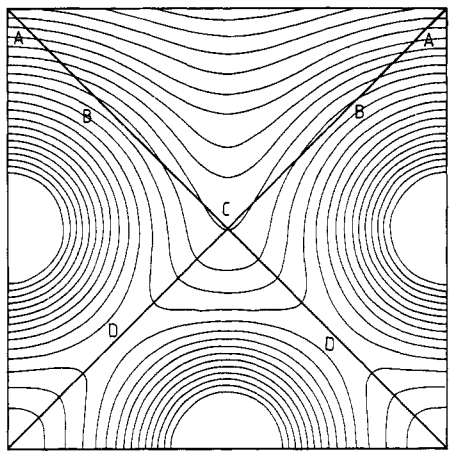

Figure 2. Self-consistent charge density for Au(100) along the (11) surface direction. As a guide to the eye, the bulk Wigner–Seitz cell boundaries are shown. Surface charge density redistribution is away from regions A and B and towards region C. The interlayer bond charge (point D) is close to the bulk value. See § 3 of text for details.

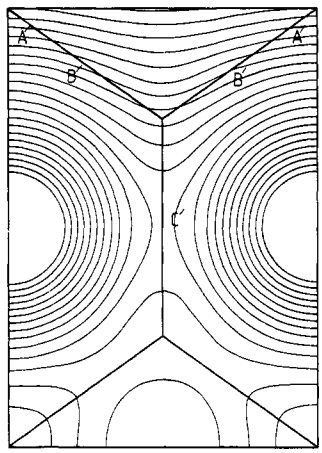

Figure 3. Self-consistent charge density plot for Au(100) along the (10) surface direction. The surface charge density flows away from regions A′ and B′ while the bond charge density C′ is increased. See § 3 of text for details.

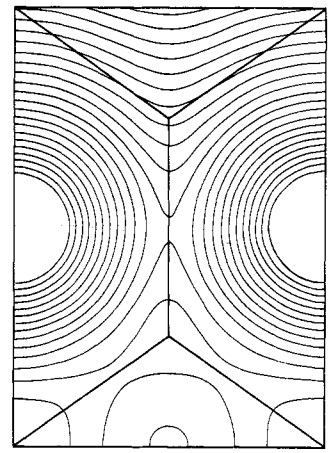

Figure 4. Superposed atomic charge density for Au(100) along the (10) direction, for comparison with figure 3 (see § 3 of text).

charge that has moved out of these areas has moved into the hollows in the surface, (area C in figure 2). A close inspection also reveals an increased charge in area C′ (in figure 3) between the surface atoms, which we shall discuss further below. We see that the overall charge movement is away from the top part of the surface atom and into the hollows between atoms, which is qualitatively similar to the redistribution suggested in [17]. Notice in particular that the charge flows out of region B, this occurring because in the bulk this region would contain the bond charge while here at the surface the bonds are broken. This shows a slight discrepancy with [17] in which it was argued that charge would flow into region B from region A. This difference does not affect the principal conclusions in [17] for the clean surface since the charge movement tangentially is still consistent with tensile surface stresses and the charge flow normal to the surface is still consistent with inward relaxation of the surface layer. The conclusions at step sites may

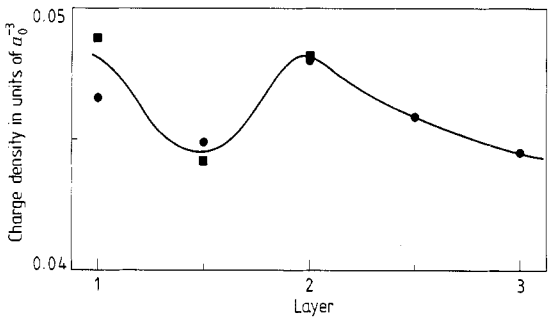

Figure 5. Bond mid-point charge density as a function of distance from the surface. The surface and second layer bonds are enhanced relative to the bulk. Calculations with both a two- and a three-atom surface region are shown as squares and circles, respectively. The curve is purely a guide for the eye.

be different, however. Our self-consistent calculations have thus confirmed the general arguments [17] at least from the clean surface. We shall make these ideas of charge redistribution and the relationship to surface stress more quantitative in § 4.

4. Enhancement of the surface-bond order on Au(100)

In this section we shall show explicitly from the surface charge density that the bonding in the surface layer is increased, and we shall also demonstrate how this relates directly to a tensile surface stress. In density-functional, total-energy calculations the surface stress can be split into kinetic, Coulomb and exchange-correlation terms; however this division is not physically very helpful for gold. A more useful description in terms of the bonding can be found by adopting a local orbital basis, which gives a division of the stress into contributions due to the various bonds present. This division follows naturally from the tight-binding expression for the Hellmann–Feynman force between two atoms i and j

$$F_{ij} = -2 \sum_{\alpha\beta} B_{\alpha\beta} \frac{\partial H_{\alpha\beta}}{\partial R_{ij}} \tag{4}$$

where indices α and β run over all orbitals of atoms i and j respectively. $H_{\alpha\beta}$ are matrix elements of the Hamiltonian, and $B_{\alpha\beta}$ is the bond order defined by

$$B_{\alpha\beta} = \frac{-1}{\pi} \operatorname{Im} \int_{-\infty}^{\varepsilon_f} \mathrm{d}\varepsilon \, [(\varepsilon - \hat{H})^{-1}]_{\alpha\beta} \tag{5}$$

where ε_F is the Fermi energy and the integral is taken infinitesimally above the real axis. The bond order is easy to interpret: it is unity for a bonding pair of states, zero for a non-bonding pair and minus one for an antibonding pair. The corrresponding contributions to the forces are attractive, zero or repulsive, respectively, (assuming $\partial H_{\alpha\beta}/\partial R_{ij}$ positive, as is usually the case). The charge density at the mid-point of the bond, ρ_b, is also simply related to the bond order, for example for identical s states $\varphi(r)$ on each atom with half-occupancy: $\rho_b = (2B + 2)|\varphi(R_{ij}/2)|^2$, which is easy to confirm for the bonding, non-bonding and anti-bonding cases. We can now combine these definitions to show how the bond charge visible in the charge density translates directly into attractive forces between the atoms.

In order to demonstrate explicitly how the interatomic bonding varies near the surface, we have plotted in figure 5 the value of ρ_b, the charge density at the midpoint of each bond, as a function of distance from the surface. We can see that the bond charge-

density is significantly increased within the first and second layers relative to the bulk-like bonds deep in the solid. From the above discussion it is clear that the bond orders and hence also the attractive interatomic forces will be much enhanced compared to their bulk values. It is this increase in attractive s–p bonding at the surface while the d repulsion remains constant that gives rise to the contractive surface stresses present on Au(100).

A crude estimate of the magnitude of the surface stress due to such an enhanced surface bond-order can be made as follows. Firstly it is necessary to know the relative contribution to the LAPW charge density due to the d and s–p electrons. This can be estimated by considering the atomic and ionic charge densities for gold. A superposed atomic density calculation gives a charge density at the bond mid-point of $0.0376a_0^{-3}$, while a superposition of Au^+ ion densities gave $0.0255a_0^{-3}$. Assuming these numbers represent the non-bonding and d-only contributions, respectively, we calculate a bond order of approximately 0.9–1.0 in the surface plane and $\simeq 0.6$ in the bulk. In order to translate these numbers into forces, we need to know the derivative of the matrix element $\partial H_{\alpha\beta}/\partial R_{ij}$. A simple way to estimate this is to note that in the bulk, the attractive bonding forces, F_s, must be counterbalanced by the d–d repulsion, F_d. An estimate of the d–d repulsive pressure [20] gave approximately 130 kbar at the equilibrium volume, and therefore $-F_s = F_d \simeq 0.24$ eV Å^{-1}. The net force is zero in all bonds except those in the top two layers for which the s–p bonding term is increased and is stronger than the d–d repulsion. The surface s–p bonds are at a strength of approximately $1/0.6$ of $|F_s|$, giving a net force of $F = (1/0.6 - 1)F_s$ per bond within the surface and sub-surface layers. From this we calculate the stress due to each of the two top layers, which is $g = F/d$, where d is the interatomic spacing (2.8848 Å), giving a total surface stress of $g = 0.11$ eV Å^2. This crude estimate is similar to the stress on Au(111) [16] which is known to be 0.173 eV Å^2. In fact the true discrepancy is even smaller, since the density of surface bonds is higher on the (111) face than on (100). The (111) surface stress is $g = \sqrt{3}F/d$ for each layer and hence $g = 0.19$ eV Å^{-2}, assuming the same bond enhancements as for the (100) face, in very good agreement with [16].

An alternative way to look at these stresses is to split the total into separate s and d contributions. The d–d repulsion F_d in each bond leads to a tensile surface stress of $g = F_d/2d = +0.043$ eV Å^{-2} on the Au(100) face. The s only contribution to the stress is thus 0.072 eV Å^{-2}. This number is larger than the surface stress of $r_s = 3$ jellium [15] of about 0.025 eV Å^{-2}, suggesting that, unlike aluminium, the sp electrons in gold cannot be treated as nearly-free electrons.

5. Universality of surface bond enhancement

In § 4 we showed from the self-consistent charge densities of Au(100) that the bonds in the surface and sub-surface layers were substantially stronger than in the bulk. In this section we show that this phenomenon in quite general for s–p-bonded surfaces, and has the same origin as the well-known surface band narrowing effect.

For simplicity consider a single band at half filling represented by a single s orbital on each site (although the argument is more general). Now form bonding and anti-bonding linear combinations of states on a pair of neighbouring sites: $|b\rangle = (|1\rangle + |2\rangle)/\sqrt{2}$, $|a\rangle = (|1\rangle - |2\rangle)/\sqrt{2}$. The bond-order can then be expressed as the

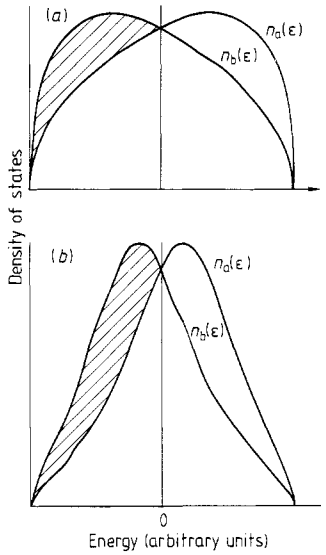

Figure 6. Origin of surface bond enhancement, showing schematically the densities of states for bonding or antibonding combinations of orbitals, with mean $+h$ and $-h$ respectively ($h < 0$). (*a*) the case of the bulk solid; (*b*) the situation in the surface layer. The integral up to the Fermi energy, of $n_b(\varepsilon) - n_a(\varepsilon)$ (shaded region) is clearly larger in (*b*), thus giving an increased bond order at the surface.

occupation of $|b\rangle$ minus that of $|a\rangle$ giving

$$B = \int_{-\infty}^{\varepsilon_F} (n_b(\varepsilon) - n_a(\varepsilon))\, d\varepsilon \tag{6}$$

where the local densities of states are

$$n_i(\varepsilon) = -(\mathrm{Im}\,\langle i|(\varepsilon - \hat{H})^{-1}|i\rangle)/\pi \tag{7}$$

for $i = a$ or b. Now we can use either the moment or the recursion method to calculate the DOS $n_i(\varepsilon)$. For our purposes, though, it is sufficient to consider the mean and width of each. The mean of the density of states is given by the recursion parameter $a_0 = \langle i|\hat{H}|i\rangle$ which is $+h$ for the bonding state and $-h$ for the antibonding state, where $h = \langle 1|\hat{H}|2\rangle$ (and usually $h < 0$). Here we are setting the diagonal site energy to zero for convenience. The bandwidth is proportional to the second recursion parameter b_0, which is of order $h\sqrt{Z}$, where Z is the effective coordination number. Z will not be very different between states a and b but will reflect the local coordination, 12 in the bulk or 8 at the surface. Consider now the case of a bond in the bulk solid; here the bonding density of states $n_b(\varepsilon)$ has its mean at energy h below the Fermi energy while the antibonding DOS $n_a(\varepsilon)$ has its mean h above. Clearly when the difference is integrated up to the Fermi level, the contribution from $n_b(\varepsilon)$ will dominate, giving a positive bond order B (as shown in the top part of figure 6). This is only to be expected, and is simply an alternative description of the origin of metallic bonding. However, consider now the case of a bond at the surface; here the coordination number Z is lower. Both densities of states $n_a(\varepsilon)$ and $n_b(\varepsilon)$ becomes more peaked about the mean in the usual surface band narrowing, illustrated schematically in figure 6. A consequence of this narrowing is that the integral of $n_b(\varepsilon)$ up to the Fermi level will be increased, while that of $n_a(\varepsilon)$ will be decreased. We thus come to the quite general conclusion that the bond order will be greater in the surface layer than in the bulk. This is the simple physical origin of the surface bond

Table 1. Bond orders for nearest neighbour bonds in a 'cannonical' FCC s-band solid, showing enhancement of surface bonds. The bond orders are calculated by the recursion method assuming nearest neighbour interactions between tight-binding s basis-functions and at half-filling.

Layer	Bond order
1	0.2791
1–2	0.2275
2	0.1944
2–3	0.2443
3	0.2138
3–4	0.1999
4	0.2300
4–5	0.2161
5	0.2108

enhancements found in the Au(100) self-consistent charge density. It is clear that surface bond enhancements will occur on a wide variety of metallic surfaces.

To illustrate this point we have calculated the bond orders for an FCC metal with simple nearest-neighbour interactions, one s orbital only per site and at half occupancy. The bond orders are shown in table 1, clearly displaying the enhanced bond order of 0.28 in the surface layer compared to 0.21 in the bulk, analogous to the gold bond-charges shown in figure 6. The similarity with the self-consistent gold calculations is only qualitative, though, since the values of B are smaller than our estimates for Au(100) and the shape of the oscillatory behaviour of B in the sub-surface layers is not correctly reproduced. Clearly the detailed band structure and the self-consistency are important for determining the precise values of the bond orders; here we seek merely to demonstrate the general trend towards surface bond-order enhancement.

One final point should be made here, which is to remark on the connection between the surface bond enhancement and the success of the 'glue' model of surface interactions. In fact they contain essentially the same physics although the bond picture relies on the Hellmann–Feynman theorem to describe the surface stress, while the glue model describes the total energy. The glue term arises naturally in any local-orbital description of an s-band solid. Following [21] the band energy can be expressed as

$$E = \sum_i \int_{-\infty}^{\varepsilon_F} \varepsilon n_i(\varepsilon)\, \mathrm{d}\varepsilon \tag{8}$$

where $n_i(\varepsilon)$ is the local density of states at site i. Assuming a single band which is close to half-filling then the contribution to the band energy at site i is proportional to $h\sqrt{Z}$, where h is the hopping matrix element and Z is the coordination number of site i. Adding in a repulsive pair overlap energy, $\phi(r_{ij})$, we naturally arrive at the glue model energy of equation 1, where the function $U(n)$ is $-\sqrt{n}$ and $\rho(r_{ij})$ is proportional to $h(R_{ij})^2$. Differentiating, the glue term gives a contribution to the force in a given bond proportional to $-1/\sqrt{n}$. This implies that at the surface the bond forces due to the glue term are increased relative to the bulk, since n (or Z) is smaller. This increased attractive force corresponds precisely to the surface bond enhancements described above and has the same physical origin, namely the surface band narrowing. We thus see that this simple glue model gives an attractive surface stress which is consistent with the self-

consistent calculations and which thus explains the success of the empirical glue model calculations of [8] in describing the Au(100) reconstruction.

6. Conclusion

In conclusion, we have presented self-consistent charge density calculations for Au(100) which are consistent with the general picture of charge redistribution given in [17]. The calculated charge density clearly shows an increased bond charge in the surface relative to the bulk. By a local-orbital form of the Hellmann–Feynman theorem this increased surface bond-order shows that there are stronger attractive bonding forces in the surface layer and thus there is a tensile surface stress. The estimated strength of this stress is consistent with total energy calculations. We also show that this enhancement of surface bonds is a quite general feature of surface electronic structure related to the band narrowing, and that this effect is implicitly included in the 'glue model'.

Acknowledgments

We thank M Foulkes, V Heine and R J Needs for important discussions, and R J Blake for computational support. This work is supported by Emmanuel College Cambridge and by National Science Foundation Grant number NSF-DMR-96 12860.

References

[1] Copel M and Gustafsson T 1986 *Phys. Rev. Lett.* **57** 723
[2] Harten U, Lahee A M, Toennies J P and Wöll C 1985 *Phys. Rev. Lett.* **54** 2619
[3] Rieder K H, Engel T, Swendsen R H and Manninen M 1983 *Surf. Sci.* **127** 223
[4] Yamazaki K, Tagayanagi K, Tanshiro Y and Yagi Y 1988 *Surf. Sci.* **199** 595
[5] Fedak D G and Gjostein N A 1967 *Surf. Sci.* **8** 77
[6] van Hove M A, Koestner RJ, Stair PC, Bibérìan JD, Kesmodel LL, Bartoš I and Somorjai GA 1981 *Surf. Sci.* **103** 189
[7] Binnig G K, Rohrer H, Gerber C and Stoll E 1984 *Surf. Sci.* **144** 321
[8] Ercolessi F, Tosatti E and Parrinello M 1986 *Phys. Rev. Lett.* **57** 719
Ercolessi F, Parrinello M and Tosatti E 1986 *Surf. Sci.* **177** 314
[9] Garofalo M, Tosatti E and Ercolessi F 1987 *Surf. Sci.* **188** 312
[10] Daw M S 1986 *Surf. Sci.* **166** L161
[11] Sowa E C, Van Hove M A and Adams D L 1988 *Surf. Sci.* **199** 174
[12] Jacobsen K W and Nørksov J K 1987 *Springer Series in Surface Science* vol 11, p 118 (Berlin: Springer)
[13] Ho K M and Bohnen K P 1987 *Europhys. Lett.* **4** 345
Ho K M and Bohnen K P 1987 *Phys. Rev. Lett.* **59** 1833
[14] Nielsen O H and Martin R M 1985 *Phys. Rev.* B **32** 3780
[15] Needs R J 1987 *Phys. Rev. Lett.* **58** 53
Needs R J and Godfrey M J 1987 *Phys. Scr.* **19** 391
[16] Payne M C, Roberts N, Needs R J, Needels M and Joannopoulos J D 1988 *Preprint*
[17] Heine V and Marks L D 1986 *Surf. Sci.* **165** 65
[18] Benesh G A and Inglesfield J E 1984 *J. Phys. C: Solid State Phys.* **17** 1595
Inglesfield J E and Benesh G A 1988 *Phys. Rev.* B **37** 6682
[19] Gallagher J M and Haydock R 1978 *Phil. Mag.* B **38** 155
[20] Christensen N E and Heine V 1985 *Phys. Rev.* B **32** 6145
[21] Finnis M W and Sinclair J E 1984 *Phil. Mag.* A **50** 45